Astron. Astrophys. 360, 272–280 (2000)

ASTRONOMY AND ASTROPHYSICS

# The long-period RS CVn binary IM Pegasi

## II. First surface images*

**S.V. Berdyugina[1], A.V. Berdyugin[1,2], I. Ilyin[1], and I. Tuominen[1]**

[1] Astronomy Division, P.O. Box 3000, 90014 University of Oulu, Finland
[2] Tuorla Observatory, University of Turku, Väisäläntie 20, 21500 Piikkiö, Finland

Received 10 April 2000 / Accepted 25 May 2000

**Abstract.** New high-resolution, high signal-to-noise ratio spectroscopic observations and UBV photometry carried out in 1996–1999 were analysed with the surface imaging technique. A total of 8 images of IM Peg was obtained for the first time. A huge high-latitude active region was found to dominate the stellar surface and decreased in area during the period of the observations. At the same time, on the opposite hemisphere (in longitudes), smaller spots were developing. The spots were migrating in the orbital reference frame, the period of spot rotation being of $24\overset{d}{.}73\pm0\overset{d}{.}02$. The spots constitute two active longitudes on opposite stellar hemispheres, similar to other RS CVn stars. The evolution of the spot areas within the active longitudes indicates a stellar activity cycle, during which one active longitude dominates the stellar activity, to be about 6.5 years. Then, a total cycle, comprising two consecutive periods of activity of both active longitudes, is about 13 years. In 1999, the activity switched to the other active longitude. This declared the beginning of a new (half-) cycle.

**Key words:** stars: imaging – stars: starspots – stars: activity – stars: late-type – stars: individual: IM Peg

### 1. Introduction

We continue our study of the single-lined RS CVn-type binary IM Pegasi (HD 216489). In Paper 1 (Berdyugina et al. 1999b) we presented a detailed analysis of the photospheric spectrum of the star and determined, with high accuracy, stellar and orbital parameters. Many of those parameters are of great importance for the present study – the surface imaging of the star.

For the last decade, the technique of stellar surface imaging was extensively used for studying cool active stars with temperature inhomogeneities, i.e. spots. The most recent and vast account of images has been given by Strassmeier (2000). According to this, 208 images for 53 cool stars of different types have been obtained to date. Despite this, the processes maintaining and governing the stellar activity are still far from being understood. There are various reasons for this, the most important is the short time span covered by images and large, seasonal, gaps between them. The number of images for a given star is often too small to draw conclusions about the stellar activity as a phenomenon. In our opinion, the most fruitful way is to maintain monitoring of the most prominent targets for reasonably long times with good seasonal coverage. This will result in a series of images which can be searched for spot evolution, long-lived structures, surface differential rotation, etc. Such a tactic has already resulted in fairly interesting results for a few stars (V711 Tau, Vogt et al. 1999; II Peg, Berdyugina et al. 1998a, 1999a; EI Eri, LQ Hya, see references in Strassmeier 2000). To date, these four stars are the best studied with the surface imaging technique, with the number of images more than 10 per star.

In spite of its long period ($24\overset{d}{.}65$), we have chosen IM Peg as one of our targets for surface imaging monitoring because of its brightness ($V=5\overset{m}{.}6$) and rather prominent activity. The active component in this binary is a "normal" K2 III star with typical parameters for giants except the rapid rotation and chromospheric activity (see Paper 1). From time to time, generally since 1970, but more regularly since 1991, IM Peg was observed photometrically (see compilation by Strassmeier et al. 1997). In 1991, the star significantly reduced its mean brightness (by $0\overset{m}{.}15$ in $V$) and, being at this level, demonstrated the largest ever observed amplitude of the variability in the fall of 1995 ($\Delta V=0\overset{m}{.}36$). We started our spectroscopic observations 8 months later, in summer 1996, when the amplitude was still large ($0\overset{m}{.}32$). Here, we present the first images of IM Peg for 4 years, 1996–1999, two images per year. We trace the spot evolution during the decrease of the amplitude of the photometric wave and find evidence for long-lived spot structure.

### 2. Observations

Spectroscopic observations were carried out in 1996 with the 2.6 m telescope of the Crimean Astrophysical Observatory and in 1997–1999 with the 2.56 m Nordic Optical Telescope (NOT), La Palma. The spectral resolving power $\lambda/\Delta\lambda$ in the region of

*Send offprint requests to*: S.V.Berdyugina (sveta@ukko.oulu.fi)

* based on observations collected at the Nordic Optical Telescope (NOT), La Palma, Spain; the 2.6 m and 1.25 m telescopes of the Crimean Astrophysical Observatory, Ukraine; the 2m telescope of the National Astronomical Observatory, Rozhen, Bulgaria.

**Table 1.** Spectroscopic observations used for surface imaging.

| HJD 2450000+ | Phase | S/N | HJD 2450000+ | Phase | S/N | HJD 2450000+ | Phase | S/N | HJD 2450000+ | Phase | S/N |
|---|---|---|---|---|---|---|---|---|---|---|---|
| *1996* | | | *1997* | | | *1998* | | | *1999* | | |
| 320.3855 | 0.087 | 315 | 617.7301 | 0.151 | 310 | 997.6590 | 0.564 | 180 | 1325.7350 | 0.874 | 220 |
| 324.4004 | 0.250 | 210 | 618.6970 | 0.190 | 215 | 998.6667 | 0.605 | 275 | 1327.7438 | 0.956 | 155 |
| 325.4121 | 0.291 | 290 | 619.7147 | 0.231 | 240 | 999.6650 | 0.646 | 280 | 1328.7463 | 0.996 | 135 |
| 326.3850 | 0.331 | 360 | 620.6416 | 0.269 | 305 | 1000.6429 | 0.685 | 215 | 1329.7395 | 0.037 | 120 |
| 327.4263 | 0.373 | 265 | 621.7115 | 0.312 | 250 | 1001.6495 | 0.726 | 255 | 1330.7393 | 0.077 | 220 |
| 331.3644 | 0.533 | 400 | 622.6684 | 0.351 | 240 | 1002.6552 | 0.767 | 215 | 1331.7412 | 0.118 | 180 |
| 348.2273 | 0.217 | 295 | 623.6664 | 0.391 | 210 | 1003.6596 | 0.808 | 250 | 1332.7375 | 0.158 | 205 |
| 353.2663 | 0.421 | 310 | 624.6193 | 0.430 | 295 | 1004.6544 | 0.848 | 295 | 1333.7358 | 0.199 | 215 |
| 357.3160 | 0.586 | 370 | 625.6403 | 0.471 | 340 | 1005.6522 | 0.888 | 295 | 1383.7155 | 0.226 | 205 |
| 359.2699 | 0.665 | 350 | 626.6596 | 0.513 | 305 | 1006.6487 | 0.929 | 205 | 1384.7146 | 0.267 | 270 |
| 360.2654 | 0.705 | 430 | 627.6485 | 0.553 | 320 | 1008.6667 | 0.011 | 250 | 1385.7056 | 0.307 | 210 |
| 364.3888 | 0.872 | 360 | 676.6865 | 0.542 | 330 | 1009.6586 | 0.051 | 240 | 1386.7218 | 0.348 | 180 |
| 365.4010 | 0.914 | 305 | 677.7371 | 0.585 | 290 | 1088.5102 | 0.250 | 310 | 1387.7151 | 0.389 | 225 |
| 376.2793 | 0.355 | 395 | 678.7044 | 0.624 | 325 | 1089.3766 | 0.285 | 255 | 1388.7033 | 0.429 | 230 |
| 401.1248 | 0.363 | 410 | 679.7209 | 0.665 | 310 | 1090.4230 | 0.328 | 260 | 1389.7211 | 0.470 | 180 |
| 402.1285 | 0.404 | 390 | 680.7073 | 0.706 | 280 | 1091.3660 | 0.366 | 260 | 1390.7042 | 0.510 | 200 |
| 403.1255 | 0.444 | 380 | 681.6938 | 0.746 | 290 | 1092.3800 | 0.407 | 230 | 1391.6966 | 0.550 | 250 |
| 404.1280 | 0.485 | 400 | 682.6980 | 0.786 | 300 | 1093.3910 | 0.448 | 270 | 1392.6997 | 0.591 | 255 |
| 405.1257 | 0.525 | 300 | 683.7280 | 0.828 | 255 | 1094.4126 | 0.489 | 220 | 1393.6838 | 0.631 | 225 |
| 406.1570 | 0.567 | 420 | 735.5393 | 0.930 | 250 | 1095.5023 | 0.533 | 195 | 1394.7098 | 0.672 | 230 |
| 407.1349 | 0.607 | 405 | 736.5674 | 0.972 | 280 | 1096.5326 | 0.575 | 80 | 1443.5138 | 0.652 | 240 |
| 408.2645 | 0.653 | 360 | 737.3925 | 0.005 | 400 | 1097.5870 | 0.618 | 160 | 1444.5111 | 0.692 | 210 |
| 409.1188 | 0.687 | 420 | 794.2832 | 0.313 | 290 | 1121.4344 | 0.586 | 220 | 1445.5514 | 0.735 | 215 |
| 410.2835 | 0.734 | 270 | 795.3391 | 0.356 | 450 | 1122.4017 | 0.625 | 240 | 1447.5424 | 0.816 | 200 |
| 412.1521 | 0.810 | 410 | 796.3377 | 0.397 | 220 | 1123.3838 | 0.665 | 250 | 1449.5606 | 0.898 | 155 |
| 413.1524 | 0.851 | 190 | 797.3694 | 0.438 | 160 | 1124.3835 | 0.705 | 220 | 1471.6012 | 0.792 | 200 |
| 414.1480 | 0.891 | 425 | 802.3858 | 0.642 | 240 | 1125.3957 | 0.746 | 240 | 1472.6078 | 0.833 | 230 |
| 415.1713 | 0.933 | 295 | 804.3154 | 0.720 | 245 | 1126.4442 | 0.789 | 180 | 1473.6223 | 0.874 | 170 |
| 417.1289 | 0.012 | 350 | 805.3051 | 0.760 | 310 | 1127.4384 | 0.829 | 210 | 1475.5391 | 0.952 | 200 |
| 418.1573 | 0.054 | 300 | 806.3182 | 0.802 | 220 | | | | 1481.2978 | 0.185 | 245 |
| 420.1373 | 0.134 | 240 | | | | | | | 1482.4048 | 0.230 | 250 |
| 421.1315 | 0.175 | 270 | | | | | | | 1483.2762 | 0.266 | 235 |
| 423.3231 | 0.263 | 110 | | | | | | | 1484.3012 | 0.307 | 205 |
| | | | | | | | | | 1485.2855 | 0.347 | 215 |
| | | | | | | | | | 1505.2851 | 0.158 | 200 |
| | | | | | | | | | 1509.3069 | 0.322 | 240 |

the lines used for surface imaging (6180 Å) was about 40 000 and 80 000, respectively. Other details of the quality of the observations with the two telescopes have been given in Paper 1. Additionally, in 1999, 5 spectra were obtained with the 2 m telescope of the National Astronomical Observatory, Rozhen, Bulgaria, with the resolving power of about 30 000.

In 1996, the observations were carried out in August-October (JD2450320–376) and November-December (JD245401–423). These provided two sets with a good phase coverage, 14 and 19 phases, respectively.

In 1997, the observations were carried out in June, August, October and December. We divided these observations into two slightly overlapping sets: June–October (JD2450617–737) and October–December (JD2450735–806). The first set has an excellent phase coverage (22 phases), while the second has a phase gap from 0.0 to 0.3.

In 1998, a total of 31 phases has been obtained in July, October and November. These constituted two overlapping sets: JD2450997–1094 and JD2451005–1127. This provided an acceptable phase coverage for both sets, with gaps of only about 0.2.

In 1999, 36 phases had been obtained in the period from the end of May to the end of November. Again, we were not able to avoid overlapping because of missing important phases in some months. Two sets were created as follows: May–September (JD2451325–1449) and August–November (JD2451388–1509). In the second set, the observations from the NOT and Rozhen Observatory were combined, accounting for the different instrumental profiles.

All observations were phased according to the orbital ephemeris from Paper 1, which is used throughout this paper:

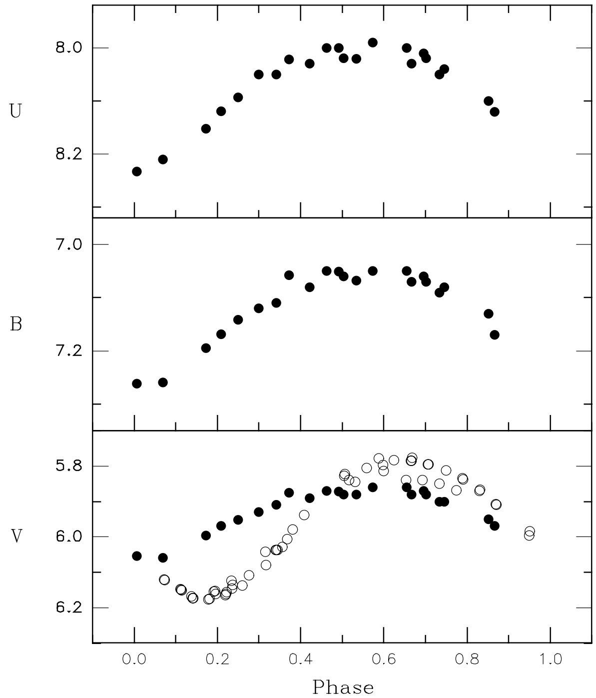


**Fig. 1.** UBV observations of IM Peg in August-September 1997 (dots; present paper) and in Nov-Dec 1996 (open circles; Strassmeier et al. 1999). The data are phased with the ephemeris given by Eq. (1).

$$\mathrm{T_{conj}} = 2\,450\,342.883 + 24.64880\,E \quad (1)$$

with the primary in the back at phase zero. Heliocentric Julian dates, orbital phases, and S/N ratios of the spectra used for surface imaging are presented in Table 1.

Supporting photometric observations were arranged in August–September 1997 with the photometer-polarimeter installed on the 1.25 m telescope of the Crimean Astrophysical observatory (Piirola 1973). The observations were carried out in the standard UBV system with HD 216635 as a comparison star (U=$8^{\mathrm{m}}_{.}34$, B=$7^{\mathrm{m}}_{.}60$, V=$6^{\mathrm{m}}_{.}56$). The observations are presented in Table 2 and Fig. 1. For the fall of 1997 we used observations published by Strassmeier et al. (1999), while for other seasons no photometric observations have yet been published.

**Table 2.** Photometric observations

| HJD 2450000+ | Phase | U | B | V |
|---|---|---|---|---|
| 663.4800 | 0.0047 | 8.232 | 7.262 | 6.055 |
| 667.5468 | 0.1696 | 8.152 | 7.195 | 5.997 |
| 668.4558 | 0.2065 | 8.119 | 7.169 | 5.969 |
| 669.4619 | 0.2473 | 8.093 | 7.141 | 5.952 |
| 672.4750 | 0.3696 | 8.022 | 7.058 | 5.876 |
| 675.4232 | 0.4892 | 8.000 | 7.051 | 5.872 |
| 676.4906 | 0.5325 | 8.021 | 7.068 | 5.880 |
| 677.4491 | 0.5714 | 7.990 | 7.050 | 5.860 |
| 679.4676 | 0.6533 | 8.000 | 7.050 | 5.860 |
| 680.4500 | 0.6931 | 8.010 | 7.060 | 5.870 |
| 681.4024 | 0.7318 | 8.050 | 7.090 | 5.900 |
| 684.3131 | 0.8499 | 8.100 | 7.130 | 5.950 |
| 695.3505 | 0.2976 | 8.050 | 7.120 | 5.930 |
| 696.3652 | 0.3388 | 8.050 | 7.110 | 5.910 |
| 698.3590 | 0.4197 | 8.030 | 7.080 | 5.890 |
| 699.3517 | 0.4600 | 8.000 | 7.050 | 5.870 |
| 700.3553 | 0.5007 | 8.020 | 7.060 | 5.880 |
| 704.4002 | 0.6648 | 8.030 | 7.070 | 5.880 |
| 705.2732 | 0.7002 | 8.020 | 7.070 | 5.880 |
| 706.3231 | 0.7428 | 8.040 | 7.080 | 5.900 |
| 709.3124 | 0.8641 | 8.120 | 7.170 | 5.970 |
| 714.3163 | 0.0671 | 8.210 | 7.260 | 6.060 |

**Table 3.** Atmospheric parameters of the primary of IM Peg used for surface imaging (from Paper 1).

| Parameter | Value |
|---|---|
| $\mathrm{T_{eff}}$, K | 4450 |
| log $g$ | 2.4 |
| [M/H] | 0.0 |
| $\xi_{\mathrm{t}},\ \mathrm{km\,s^{-1}}$ | 1.6 |
| $\zeta_{\mathrm{t}},\ \mathrm{km\,s^{-1}}$ | 4.0 |
| $v\,\sin i,\ \mathrm{km\,s^{-1}}$ | 26.5 |
| $i$ | 70° |

## 3. Surface imaging

### 3.1. Local line profiles

We have chosen the 6160–6200 Å region as the region for surface imaging of K giants and subgiants. It contains Fe I, Ni I and V I lines which are strong enough but not yet saturated and have different temperature sensitivities. We found that for proper temperature imaging, the combination of Ni I and V I lines is very useful, since their intensities change in opposite directions with changing temperature, and this strongly constrains the solution. These lines were previously used for surface imaging of the RS CVn-type star II Peg (Berdyugina et al. 1998a, 1999a).

A list of atomic line parameters was obtained from VALD (Piskunov et al. 1995, Kupka et al. 1999) for lines having a central depth of 1% or more. A number of molecular lines were included in the list. The line list was previously tested using the $\beta$ Gem (K0 IIIb) spectrum as was reported by Berdyugina et al. (1998b). A set of local line profiles for the temperature range of 3500–6000 K and ten limb angles on the stellar disk was calculated using the stellar atmosphere models by Kurucz (1993) and the parameters of the atmosphere obtained in Paper 1 and presented in Table 3. The instrumental profiles were approximated by the Gaussian functions with a width corresponding to the resolution of the given spectrograph. The code used for synthetic spectrum calculations was described in detail by Berdyugina (1991).

### 3.2. Images

For the inversion of the line profiles to the stellar images the Occamian approach was used (Berdyugina 1998). The approach does not use any artificial constraints for finding a unique and smooth solution. It allows also for a convenient estimation of the

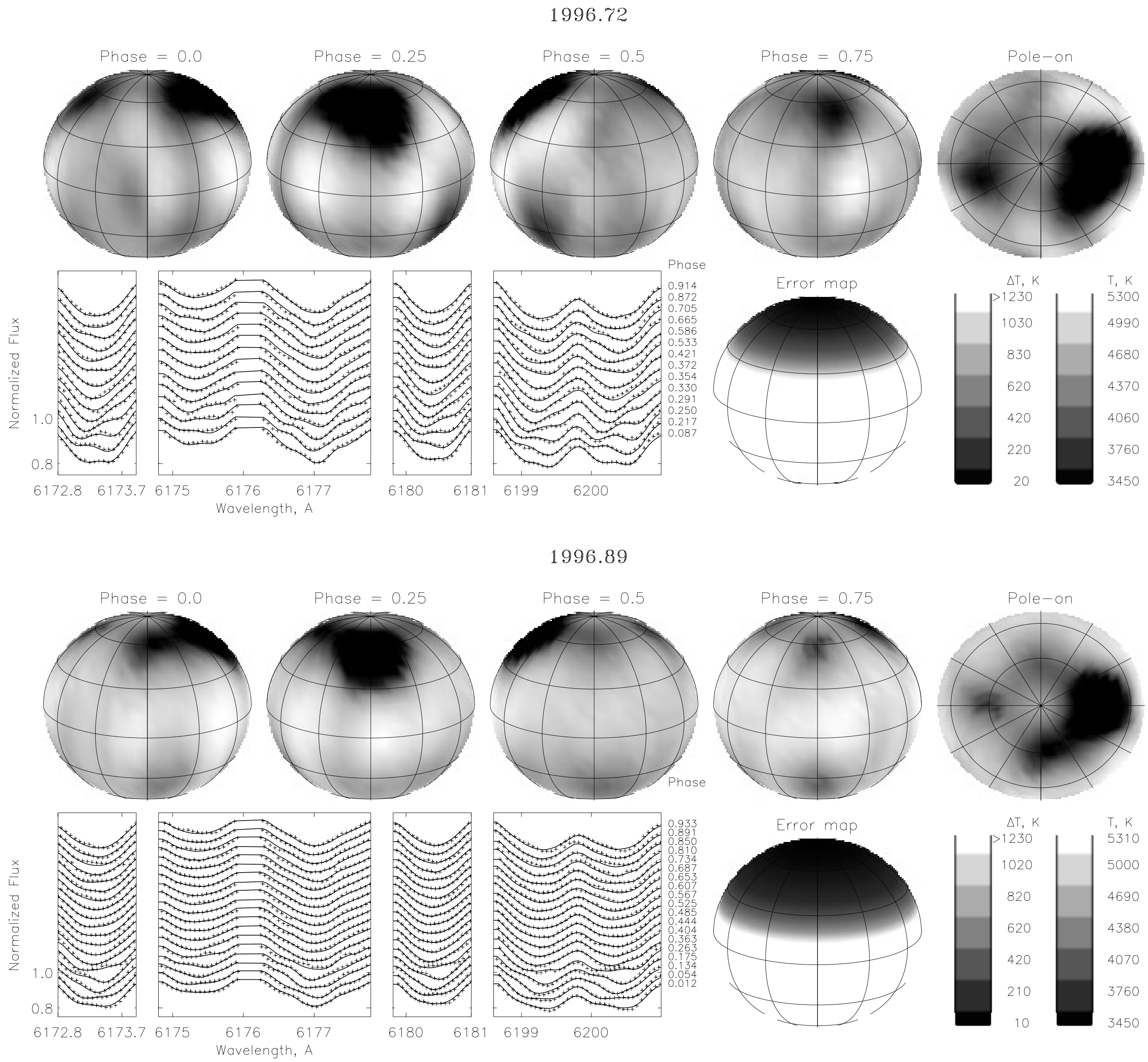


**Fig. 2.** Images of IM Peg for 1996–1999 shown for four orbital phases and also in the pole-on projection and fits to the line profiles (symbols are observations, and lines are calculations). The error maps show the distributions of the temperature errors, averaged in longitudes. Images are shown with a coordinate grid of 30° in both latitude and longitude and with the inclination of the rotation axis of 70° as was adopted in the calculations.

variances of the resulting solution. Recently, it was successfully used for surface imaging of II Peg (Berdyugina et al. 1998a, 1999a) and FK Com (Korhonen et al. 1999). In a recent paper (Berdyugina et al. 1999a) we also tested the stability of the images to the choice of spectral lines. We showed that significant spot features are seen in all strong and temperature sensitive lines, and the best map is obtained when all lines are used in inversions simultaneously. Thus, we showed that our maps are free from systematic errors, and spots seen in the maps result from real spectral features observed in the line profiles rather than from misfits between models and observations.

A grid of $6^\circ \times 6^\circ$ on the stellar surface was used for integrating the local line profiles to normalized flux profiles. With a given set of stellar atmosphere models, the stellar image is considered as the distribution of effective temperature across the stellar surface. Obviously, the resulting temperature scale of the images is model dependent. To test the temperature scale of the images, we used our photometric observations for 1997 (Table 2) and those by Strassmeier et al. (1999) for 1996. Unfortunately, no photometry is published for the years 1998 and 1999. We calculated the B–V and V–R colour indices, transforming the temperatures to the colours with the calibration for

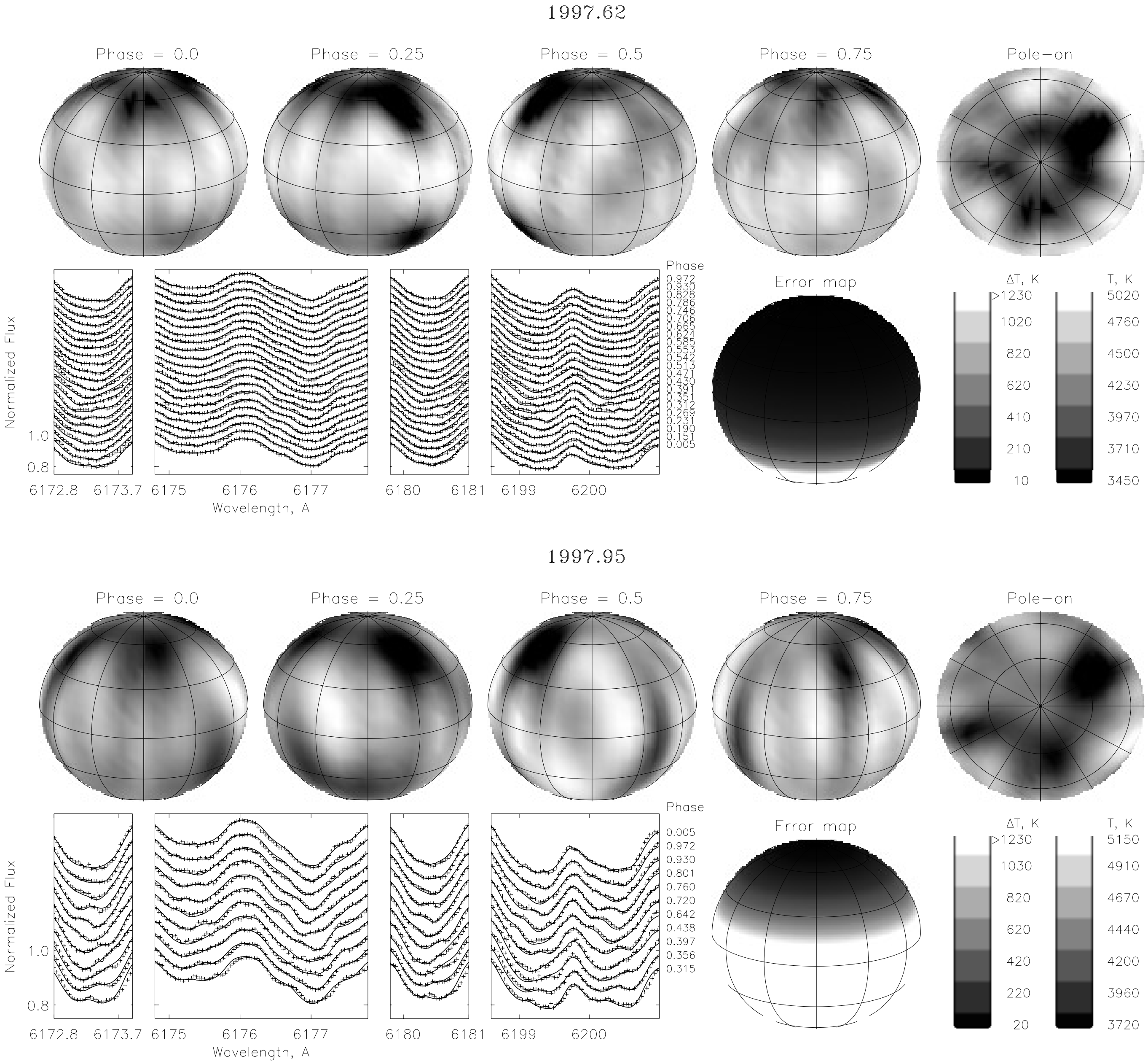


**Fig. 2.** (continued)

evolved giants by McWilliam (1990). The calculated mean values and amplitudes of the colour indices were compared with the photometric observations.

Fig. 2 displays images of IM Peg, error distributions over the stellar surface for each season, and fits to the line profiles. As was indicated, the images for the years 1997, 1998 and 1999 are partly overlapping in phases within a given season. This allowed us to obtain full-surface maps spanning a few months and, thus, to study the spot evolution on this time scale. We found that the temperature scales of the images and the spot distributions fit satisfactorily both mean values and amplitudes of the colour indices: V–R for 1996 and B–V for 1997 (Fig. 3). This provides an independent test of the images. A small difference between the observed and calculated colour indices for the 1996.89 image at the maximum brightness is caused probably by underestimating the contrast of the spot at phase 0.75. This spot is more prominent in the previous image, 1996.72.

As was mentioned, the Occamian approach supplies error estimates of the solution, which constitute lower limits of the true errors (see e.g. Berdyugina 1998). For high-quality observations (high signal-to-noise and large amount of observations), this estimates are comparable with the standard deviations, which can be determined if several maps obtained from different spectral lines are averaged (Berdyugina et al. 1999a). This indicates the stability of the solution to external errors. The accuracy of the temperature values decreases toward lower lat-

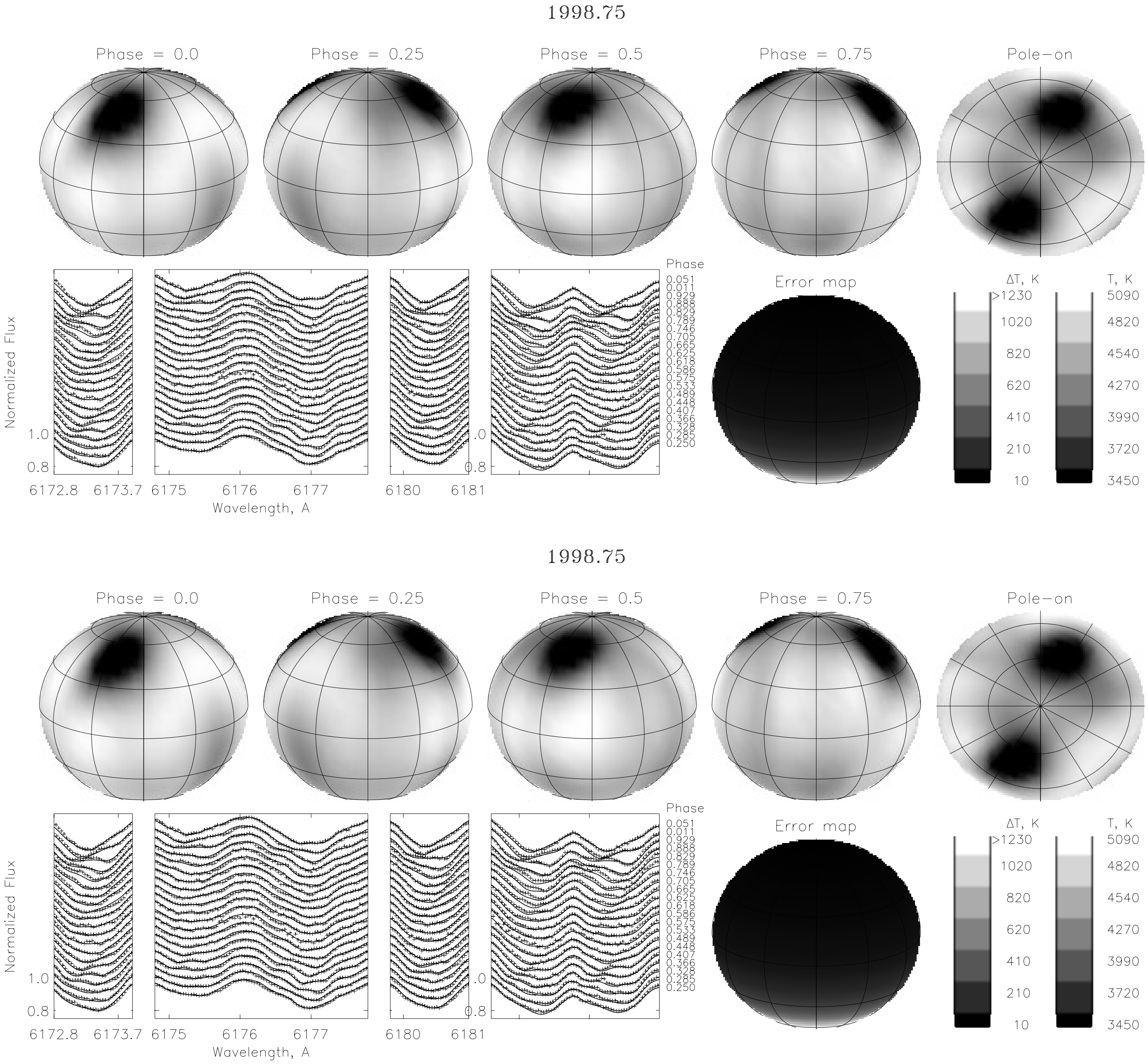


**Fig. 2.** (continued)

itudes (see Fig. 2). Thus, high-latitude spots are restored with better accuracy. Note, however, that for five images, the quantity of the observations used is quite sufficient for restoring even the equatorial regions where no spots were recovered. In those images the errors at the equator are of $\sim$200 K and smaller in the upper latitudes.

## 4. Spot evolution

### *4.1. Spot parameters*

We started our spectroscopic observations a few months after the largest amplitude in V-band was observed in the end of 1995. A huge active region at phase 0.25, seen in the first stellar image, 1996.72, seems to be the one which was responsible for the large amplitude. Since the photometric amplitude was slightly reduced during these months, the size of the region can be expected to have been even larger at its maximum. During the period of observations the size of the region has significantly diminished, while in the opposite hemisphere (in longitudes) smaller spots were constantly developing. Photometric observations for the seasons show a decrease of the amplitude in the V-band from $0\overset{\mathrm{m}}{.}3$ in 1996 (Strassmeier et al. 1997, 1999) to $0\overset{\mathrm{m}}{.}22$ in 1997 (our observations). Also, the brightness maximum decreased by $0\overset{\mathrm{m}}{.}05$ (see Fig. 1). This clearly confirms the observed spot evolution. The light curve amplitude in 1998 should have

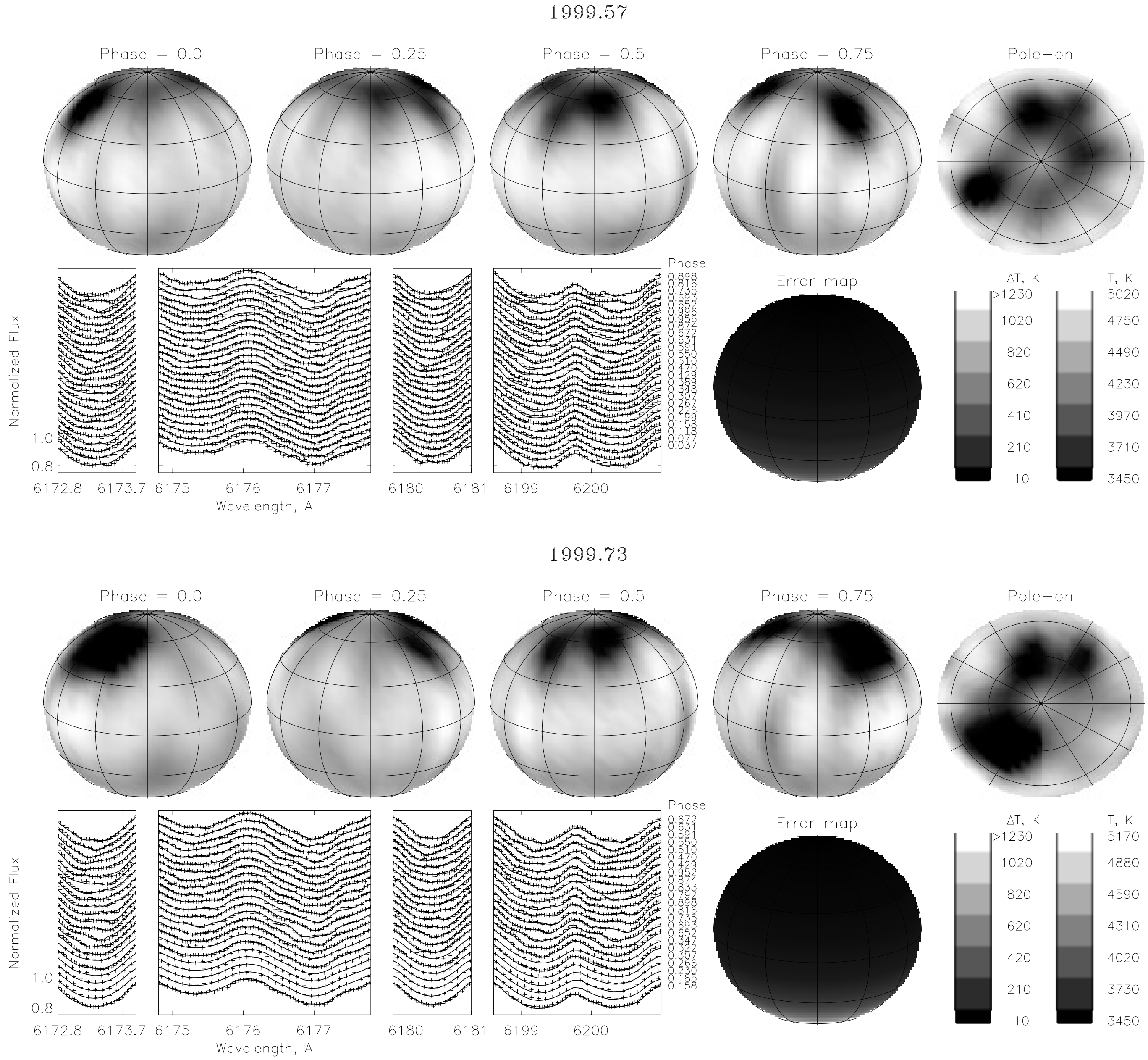


**Fig. 2.** (continued)

been lower, however no photometric observations are available to us.

In Table 4 we present the spot parameters measured from the maps: phase, the moment of passing the central meridian and the projected spot area in percentage of the stellar disk area. Phases of spots were measured from the parabolic fits to minima of the temperature distribution averaged over the spot latitudes. The moments in Julian days were calculated from the phases with the ephemeris given by Eq. (1) as the closest times to the observations. Here, the central meridian corresponds to the conjunction when the primary is behind the secondary. Spot areas were measured as those with the temperature below 4000 K.

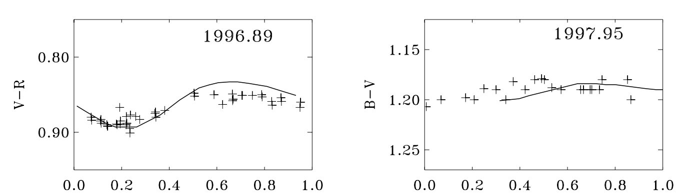


**Fig. 3.** Colour index variations: observed (crosses) and calculated from the images (lines).

One must note also that spots appear in the latitude interval of 30°–75°, with spot centres from 45° to 63°.

Note that the largest spot (Spot1, A=15.9%) has a surprisingly huge linear size, about $6.5\,R_\odot \times 10.5\,R_\odot$ with the radius

**Table 4.** Spot parameters: $\varphi$ - orbital phase, T - heliocentric Julian day at the moment of the spot passage through the central meridian minus 2450000, A - projected spot area in percentage of the stellar disk area.

| Season | | Spot 1 | Spot 2 | Spot 3 |
|---|---|---|---|---|
| 1996.72 | $\varphi$ | 0.258 | 0.775 | |
| | T | 324.594 | 361.986 | |
| | A | 15.9 | 2.6 | |
| 1996.89 | $\varphi$ | 0.258 | 0.742 | |
| | T | 423.189 | 410.470 | |
| | A | 15.1 | 1.6 | |
| 1997.62 | $\varphi$ | 0.342 | 0.958 | 0.758 |
| | T | 622.450 | 736.229 | 682.001 |
| | A | 10.9 | 3.2 | 2.4 |
| 1997.95 | $\varphi$ | 0.342 | 0.042 | 0.808 |
| | T | 794.991 | 738.299 | 806.478 |
| | A | 8.4 | 2.6 | 1.6 |
| 1998.53 | $\varphi$ | 0.425 | 0.942 | 0.292 |
| | T | 994.228 | 1006.971 | 1089.544 |
| | A | 11.4 | 6.5 | 1.9 |
| 1998.75 | $\varphi$ | 0.425 | 0.925 | |
| | T | 1092.823 | 1129.796 | |
| | A | 6.8 | 6.0 | |
| 1999.57 | $\varphi$ | 0.508 | 0.825 | 0.425* |
| | T | 1390.654 | 1324.521 | 1388.608 |
| | A | 2.6 | 6.2 | 1.3 |
| 1999.73 | $\varphi$ | 0.525 | 0.858 | 0.408 |
| | T | 1391.073 | 1448.579 | 1388.189 |
| | A | 3.6 | 11.0 | 1.6 |

* In the 1999.57 image, even four spots can be distinguished, the 4th spot having the following parameters: $\varphi$=0.275, T=1384.911, A=1.3.

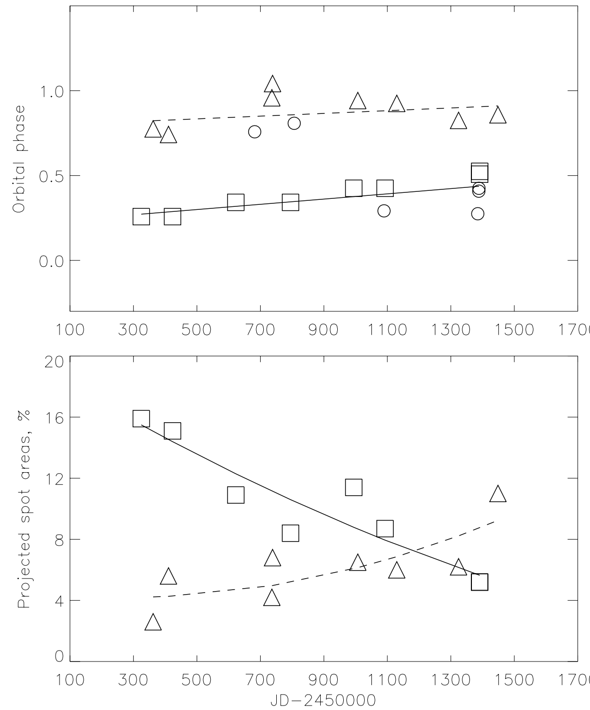


**Fig. 4.** Positions and projected areas of spots recovered in the images. Spot1, Spot2 and Spot3 from Table 4 are shown by squares, triangles and small circles, respectively. Active longitudes are shown by solid and dashed lines. In the low plot, the area of Spot3 was added to that of Spot1 or Spot2.

of IM Peg being about 13 $R_\odot$ (Paper 1). This is only two times smaller than the absolute record (HD12545, K0III, Strassmeier 1999). It is clear that such large "solid" spots should gradually dissipate, as is seen in the images of IM Peg.

### *4.2. Active longitudes*

In Fig. 4 we plot the phases and areas of the spots versus date (from Table 4) to see the spot migration and evolution. It is clearly seen that Spot1 and Spot2 are well separated by about half a period while Spot3 joins either Spot1 or Spot2. The spot positions clearly indicate two active longitudes on the stellar surface separated by about 180°, similar to other RS CVn stars (Berdyugina & Tuominen 1998; Berdyugina et al. 1999a). During the period of our observations (1996–1999) the active longitudes slightly migrated to later phases in the orbital reference frame with an average rate of about $0^\circ\!.5\,\mathrm{day}^{-1}$. The average spot period is then $24^{\rm d}\!.73\pm0^{\rm d}\!.02$. This differs significantly from the photometric period of $24^{\rm d}\!.39$ given by Strassmeier et al. (1993) and a more recent long-term average of $24^{\rm d}\!.49$ presented by Strassmeier et al. (1997). However, one must note that seasonal values of the photometric period found in the literature vary within the interval from $24^{\rm d}\!.1$ to $25^{\rm d}\!.2$. This suggests strong variations of the spot distribution from season to season.

### *4.3. Activity cycle*

If one looks at the spot area evolution within the active longitudes (lower panel in Fig. 4), more similarities to other RS CVn stars can be found. While in one active longitude the spot areas were decreasing during the observation period (Spot1), in the other they were gradually increasing (Spot2). The area of Spot3 was added to that of Spot1 or Spot2. In late 1998, the two active regions became almost the same in area and, shortly afterwards, in 1999, they altered in such a way that the dominating activity switched to the other active longitude (Spot2).

This effect has been first observed in the images of II Peg (Berdyugina et al. 1999a) and discovered in photometric light curves of four other RS CVn stars (Berdyugina & Tuominen 1998). We suggested that the moment of switching corresponds to the beginning of a new activity cycle and the time between two switches determines the length of the cycle. This was confirmed for II Peg. As for IM Peg, we probably traced about half of the cycle. Since the maximum spot area in the dominating longitude (Spot1) was expected to be near the end of 1995 (maximum observed light curve amplitude), the cycle length can be estimated to be as long as 6.5 years. Thus, this cycle probably started in the middle of 1992.

The years 1991 and 1992 were a remarkable time for IM Peg. It showed the smallest amplitude of variability and the faintest mean magnitude when compared with previous observations (see the light curves in Fig. 25 in Strassmeier et al. 1997). Two almost equal minima were observed at that time, one becoming significantly deeper afterwards. Such a light curve evolution suggests the estimate of the cycle of 6.5 yr to be rather reliable. One must note, however, that during the 6.5 yr cycle only one active longitude was dominating the activity. As was previously suggested, a *total cycle* of the stellar activity comprises two consecutive periods of activity of both active longitudes (Berdyugina & Tuominen 1998). This results in the total cycle length of IM Peg of about 13 years.

A close look at the light curves for the period from 1991 reveals another interesting fact. While the mean magnitude remains roughly constant, the maximum and minimum brightness increases and drops, respectively, almost symmetrically, and the amplitude of the variability increases. Such behaviour is possible only if a nearly constant amount of the spot area is symmetrically redistributed between two stellar hemispheres, namely between two active longitudes. Such a spot evolution is observed for many RS CVn stars. For II Peg, we showed that symmetric spot redistribution is a key process in establishing an activity cycle (Berdyugina et al. 1999a). The same conclusion can be made now for IM Peg as well.

## 5. Conclusions

New high-resolution spectroscopic observations have been used for the first surface imaging of the visible component of the RS CVn binary IM Pegasi. With the Occamian approach as an inversion technique, several line profiles were simultaneously inverted, and a total of 8 stellar images for 1996–1999 were obtained. From the analysis of the images the following conclusions can be drawn:

1. Spots appear in high and mid latitudes, in the interval of 30°–75°, with centres between 45° and 63°.
2. A huge active region at phase 0.25 is seen in the first stellar image in 1996 with a linear size of about $6.5\,R_\odot \times 10.5\,R_\odot$. It significantly diminished during the period of the observations, while in the opposite stellar hemisphere (in longitudes) smaller spots were constantly developing. This active region has presumably existed since at least 1992, reaching its maximum area in the end of 1995.
3. The spots indicate two active longitudes separated by about 180°, which were constantly migrating to later orbital phases during the years of observations. The period of the spot rotation is estimated to be $24\overset{d}{.}73 \pm 0\overset{d}{.}02$.
4. In one active longitude, the spot areas decreased during the observation period, while in the other they gradually increased. In late 1998, the two active regions became almost the same in area and in 1999 the dominating activity has switched to the other active longitude. This indicated the beginning of a new activity cycle.
5. The length of the cycle, during which one active longitude dominates the activity of IM Peg, is estimated to be 6.5 years.

*Acknowledgements.* We are thankful to Dr. Klaus G. Strassmeier for the complete set of photometric observations of IM Peg, which he kindly made available for us, and for his valuable comments to the paper. We thank Drs. R. Duemmler, I. Iliev and L. Iliev for obtaining observations with the 2m telescope of the National Astronomical Observatory, Rozhen, Bulgaria. Also, we are thankful to Dr. R. Duemmler for his useful remarks to the manuscript. Inversions were carried out on the Cray C94/128 supercomputer in the Center of Scientific Computing (Espoo, Finland). The Nordic Optical Telescope is operated on the island of La Palma jointly by Denmark, Finland, Iceland, Norway, and Sweden, in the Spanish Observatorio del Roque de los Muchachos of the Instituto de Astrofisica de Canarias.

## References

Berdyugina S.V., 1991, Izv. Krymsk. Astrofiz. Obs. 83, 102
Berdyugina S.V., 1998, A&A 338, 97
Berdyugina S.V., Berdyugin A.V., Ilyin I., Tuominen I., 1998a, A&A 340, 437
Berdyugina S.V., Jankov S., Ilyin I., Tuominen I., Fekel F.C., 1998b, A&A 334, 863
Berdyugina S.V., Berdyugin A.V., Ilyin I., Tuominen I., 1999a, A&A 350, 626
Berdyugina S.V., Ilyin I., Tuominen I., 1999b, A&A 347, 932 (Paper 1)
Berdyugina S.V., Tuominen I., 1998, A&A 336, L25
Korhonen H., Berdyugina S.V., Hackman T., et al., 1999, A&A 346, 101
Kupka F., Piskunov N.E., Ryabchikova T.A., Stempels H.C., Weiss W.W., 1999, A&AS 138, 119
Kurucz R.L., 1993, Kurucz CD No. 13
McWilliam A., 1990, ApJS 74, 1075
Piirola V., 1973, A&A 27, 383
Piskunov N.E., Kupka F., Ryabchikova T.A., Weiss W.W., Jeffrey C.S., 1995, A&AS 112, 525
Strassmeier K.G., 1999, A&A 347, 225
Strassmeier K.G., 2000, In: García López R.J., Rebolo R., Zapatero Osorio M.R. (eds.) The Eleventh Cambridge Workshop on Cool Stars, Stellar Systems, and the Sun. ASP, San Francisco, PASPC in press
Strassmeier K.G., Bartus J., Cutispoto G., Rodono M., 1997, A&AS 125, 11
Strassmeier K.G., Hall D.S., Fekel F.C., Scheck M., 1993, A&AS 100, 173
Strassmeier K.G., Serkowitsch E., Granzer Th., 1999, A&AS 140, 29
Vogt S.S., Hatzes A.P., Misch A.A., Kürster M., 1999, ApJS 121, 546